ACS APPLIED MATERIALS & INTERFACES

Research Article

www.acsami.org

Super-Adhesive Polymer–Silica Nanocomposite Layers

T. J. Wood, L. J. Ward, and J. P. S. Badyal*

Department of Chemistry Science Laboratories, Durham University, Durham DH1 3LE, United Kingdom

ABSTRACT: Atomized spray plasma deposition (ASPD) using a precursor mixture of 2-hydroxyethyl methacrylate and methacryloyl-functionalized 15 nm silica nanoparticles leads to the formation of poly(2-hydroxyethyl methacrylate)–silica nanocomposite layers. The direct application of these coatings to overlapping glass–glass joints gives rise to excellent in situ adhesion reaching 84 MPa shear bond strength and 6 GPa shear modulus prior to the onset of adherent (bulk glass) failure. This significant enhancement in interfacial adhesion arises due to the silica nanoparticle surface methacryloyl groups enhancing cross-linking throughout the nanocomposite layer.

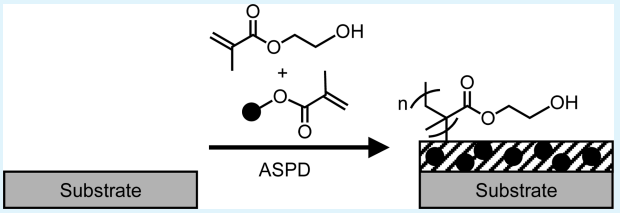

KEYWORDS: *nanocomposite, atomized spray plasma deposition, solventless adhesion, silica, nanoparticle, polymer*

1. INTRODUCTION

Poly(2-hydroxyethyl methacrylate) coatings are used for a variety of technological applications including heavy metal ion removal,[1] luminescent materials,[2,3] biomaterials,[4−6] nanostructures,[7,8] polymer electrolytes,[9] bioactivity,[10] tissue culture,[11−13] and solar cells.[14] Furthermore, the inherent biocompatibility of poly(2-hydroxyethyl methacrylate)[15] makes it a suitable adhesive for biomedical applications such as dentistry[16] and bone implants.[17] Nanocomposite variants can be formed by the addition of inorganic particles (e.g., zinc oxide,[2] calcium carbonate,[18] or silica[19−21]) to the polymer, and used for the improvement of luminescence,[2] water uptake,[21] or mechanical properties of materials.[18−20] Previous methods for preparing poly(2-hydroxyethyl methacrylate) nanocomposite layers have included sol–gel reaction,[2,19,20] free radical polymerization,[22] photopolymerization,[23,24] emulsion polymerization,[25,26] controlled radical polymerization,[27,28] in situ reduction,[29,30] and solution intercalation.[31] Such wet chemical approaches tend to require catalysts,[27] high temperatures,[20] multiple steps,[2] or long reaction times.[19]

Plasmachemical deposition of functional thin films is recognized as being a single-step, solventless, ambient temperature technique, which provides conformal coatings.[32] It has previously been shown that in the case where the electrical discharge is modulated in the presence of precursor vapor high levels of functional retention can be achieved.[33] An alternative approach for achieving such high levels of structural retention is to raise precursor vapor pressure within the reactor (i.e., increase the pressure/flow rate), such that the average plasma power per reactant molecule decreases.[32,34] However, in this case, there exist limitations due to high precursor vapor pressures/flow rates leading to plasma instabilities/inhomogeneity and eventual extinction. Such shortcomings can be overcome by utilizing an atomized spray of the precursor which limits perturbations to the plasma excitation medium by localizing the precursor molecules into concentrated fine droplets.[35,36] In this article, the use of atomized spray plasma deposition (ASPD) of 2-hydroxyethyl methacrylate–methacryloyl functionalized silica nanoparticle slurry mixtures to form highly adhesive nanocomposite layers is described, Scheme 1. The application of this one-step plasmachemical deposition process to overlapping glass–glass (or silicon–silicon) joints gives rise to excellent in situ adhesion.

Scheme 1. Atomized Spray Plasma Deposition (ASPD) of Nanocomposite Poly(2-hydroxyethyl methacrylate)–Silica Nanoparticle Layer onto Two Overlapping Substrates Leading to Penetration into the Joint and Adhesion

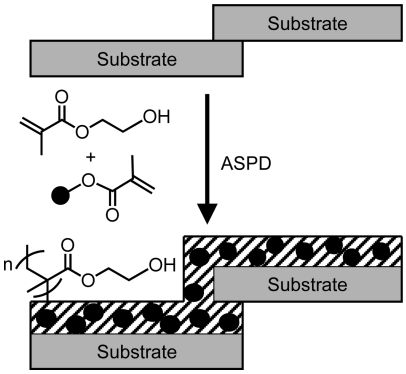

2. EXPERIMENTAL SECTION

2.1. Atomized Spray Plasma Deposition of Poly(2-hydroxyethyl methacrylate)–Silica Nanocomposite Films. Atomized spray plasma deposition was carried out in an electrodeless, cylindrical, T-shape, glass reactor (volume 820 cm^3, base pressure of 3×10^{-3} mbar, and with a leak rate better than 2×10^{-9} mol s^{-1}), enclosed in a Faraday cage, Figure 1. The atomizer precursor inlet was surrounded

Received: July 9, 2013
Accepted: September 6, 2013
Published: September 30, 2013

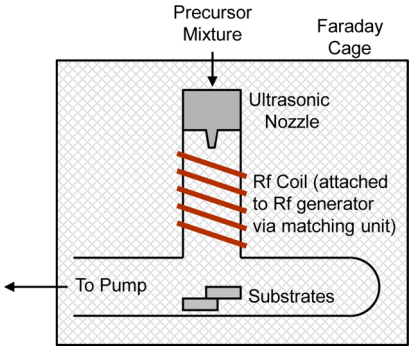

Figure 1. Atomized spray plasma deposition chamber schematic.

by a copper coil (4 mm diameter, 7 turns). The chamber was pumped down using a 30 L min^{-1} rotary pump attached to a liquid nitrogen cold trap, and a Pirani gauge was used to monitor system pressure. The output impedance of a 13.56 MHz radio frequency (rf) power supply was matched to the partially ionized gas load via an L-C matching unit connected to the copper coil. Prior to each deposition, the reactor was scrubbed with detergent, rinsed in propan-2-ol, and dried in an oven. A continuous-wave air plasma was then run at 0.2 mbar pressure and 50 W power for 30 min in order to clean any remaining trace contaminants from the chamber walls. Substrates used for coating were silicon (100) wafer pieces (Silicon Valley Microelectronics Inc.), borosilicate glass microscrope slides (Smith Scientific Ltd.), and polypropylene pieces (capacitor grade, Lawson-Mardon Ltd.). Pieces up to 45 mm diameter were placed downstream in line-of-sight from the atomizer nozzle (model no. 8700−120, Sono Tek Corp.; 25 μm diameter mean droplet size). Mixtures of 2-hydroxyethyl methacrylate (+97% Aldrich Ltd.) and methacryloyl functionalized 15 nm silica particles (Aerosil R711, Evonik Industries AG) were loaded into a sealable glass delivery tube and degassed using several freeze−pump−thaw cycles. This precursor mixture was then fed into the reactor at a flow rate of 0.02 mL s^{-1} through the ultrasonic nozzle operating at 120 kHz. Given that low input plasma power left unreacted monomer and higher power levels led to extensive plasma-induced structural degradation of the deposited layer, the optimum deposition entailed running a continuous-wave plasma at 50 W for 150 s in conjunction with precursor mixture atomization. Film thickness could be controlled by varying the period of deposition. The interaction time between the plasma zone (the length of the copper coil − approximately 10 cm) and the precursor mixture also had a bearing on the film characteristics, and therefore was kept constant. Upon plasma extinction, the system was evacuated to base pressure followed by venting to atmosphere. Deposition was carried out at ambient temperature (20 °C), and no variation in film composition was measured across the substrate. Glass, silicon wafer, and polypropylene film were all coated with uniformity and similar thickness.

2.2. Film Characterization. Surface elemental compositions were determined by X-ray photoelectron spectroscopy (XPS) using a VG ESCALAB II electron spectrometer equipped with a nonmonochromated Mg Kα X-ray source (1253.6 eV) and a concentric hemispherical analyzer. Photoemitted electrons were collected at a take-off angle of 20° from the substrate normal, with electron detection in the constant analyzer energy mode (CAE, pass energy = 20 eV). Experimental instrument sensitivity (multiplication) factors were C(1s):O(1s) equals 1.00:0.36. All binding energies were referenced to the C(1s) hydrocarbon peak at 285.0 eV. A linear background was subtracted from core level spectra and then fitted using Gaussian peak shapes with a constant full-width-half-maximum (fwhm).[37,38]

Infrared spectra were acquired using a FTIR spectrometer (Perkin-Elmer Spectrum One) fitted with a liquid nitrogen cooled MCT detector operating at 4 cm^{-1} resolution across the 700−4000 cm^{-1} range. Attenuated-total-reflection spectra were obtained using a Golden Gate accessory (Specac Ltd.).

Transmission electron microscopy (TEM) images were acquired using a Phillips CM100 microscope. This entailed embedding plasma coated polypropylene squares into an epoxy resin, and then cross-sectioning using a cryogenic microtome. The cross sections were mounted onto copper grids prior to electron microscopy analysis.

Film thicknesses were measured by freezing coated silicon samples in liquid nitrogen followed by fracture to reveal a cross-section. These were then imaged using an optical microscope (Olympus BX40) fitted with a ×20 magnification lens.

Penetration of the atomized spray plasma deposited coatings between two overlapping pieces of flat glass (1.5 mm thickness) was examined using a Raman microscope (LABRAM, Jobin Yvon Ltd.). A He−Ne laser was employed as the excitation source (632.8 nm line, operating at 20 mW). The unattenuated laser beam was focused onto the adhesive joint using a x10 microscope objective, and the corresponding Raman signals were collected by the same microscope objective in a backscattering configuration in combination with a cooled CCD detector system. The spectrometer diffraction grating (300 g/mm) was calibrated against neon light emission lines in the 600−700 nm range. The depth of coating penetration into the overlapping joint was measured by monitoring the relative intensity of the polymer C−C skeletal stretch peaks at 900−950 cm^{-1} versus distance along the joint.[39]

Adhesion testing of the atomized spray plasma deposited coatings comprised depositing directly onto two overlapping borosilicate glass microscope slide pieces. Subsequently, lap shear adhesion tests (attributable to penetration of deposited material into the joint) were carried out using an Instron 5543 tensilometer operating at a crosshead speed of 1 mm min^{-1}. At least 3 samples were tested for each composition.

3. RESULTS

3.1. Atomized Spray Plasma Deposition of Poly(2-hydroxyethyl methacrylate)−Silica Nanocomposite Films. The absence of any XPS Si(2p) signal confirmed pinhole-free surface coverage of the glass/silicon substrates following atomized spray plasma deposition of poly(2-hydroxyethyl methacrylate), Table 1. The C(1s) spectra can

Table 1. XPS Elemental Ratios for Poly(2-hydroxyethyl methacrylate) Layers

	XPS elemental ratios	
layer	%C	%O
theoretical poly(2-hydroxyethyl methacrylate)	67	33
atomized spray plasma deposited poly(2-hydroxyethyl methacrylate)	77 ± 2	23 ± 2

be fitted to three components corresponding to: hydrocarbon $\underline{C}_xH_y$ (285.0 eV), singly bonded carbon−oxygen $\underline{C}$-O (286.6 eV), and carbonyl ester O-$\underline{C}$=O (288.9 eV), Figure 2. The difference in the C(1s) envelope compared to the theoretical spectrum for poly(2-hydroxyethyl methacrylate) is consistent with plasma-induced modification at the surface of the coatings. In the case of atomized spray plasma deposition of poly(2-hydroxyethyl methacrylate)−silica nanocomposite layers, there were no discernible differences in the C(1s) XPS spectra regardless of percentage silica content (up to the maximum loading of 2.4 wt %). This is most likely due to the encapsulation of the surface silica particles with poly(2-hydroxyethyl methacrylate) polymer during deposition (XPS only probes the outermost 5 nm[40]).

The following infrared assignments are characteristic of 2-hydroxyethyl methacrylate monomer:[41] antisymmetric CH_3 stretch (2953 cm^{-1}), antisymmetric CH_2 stretch (2928 cm^{-1}), symmetric CH_3 stretch (2881 cm^{-1}), carbonyl C=O

dx.doi.org/10.1021/am402731x | ACS Appl. Mater. Interfaces 2013, 5, 9678−9683

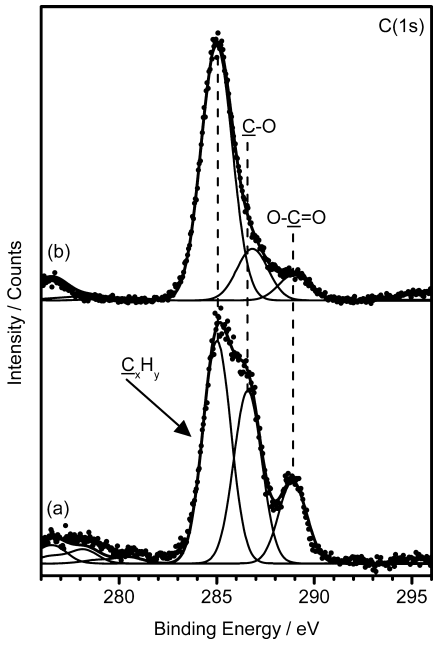

Figure 2. X-ray photoelectron C(1s) spectra of: (a) theoretical poly(2-hydroxyethyl methacrylate), and (b) atomized spray plasma deposited poly(2-hydroxyethyl methacrylate).

stretch (1713 cm^{-1}), vinyl C=C stretch (1635 cm^{-1}), $=CH_2$ wag (941 cm^{-1}), and $=CH_2$ twist (814 cm^{-1}), Figure 3.

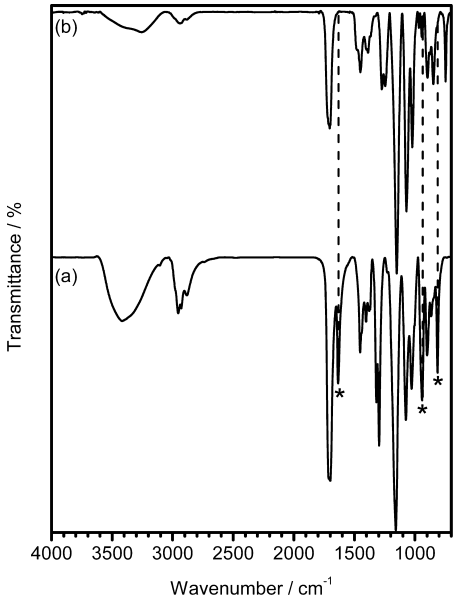

Figure 3. Infrared spectra of: (a) 2-hydroxyethyl methacrylate monomer; and (b) atomized spray plasma deposited poly(2-hydroxyethyl methacrylate) film. * Denotes absorbances associated with the polymerizable C=C double bond contained in the monomer.

Atomized spray plasma deposited poly(2-hydroxyethyl methacrylate) layers show similar absorbances except for the absence of peaks due to C=C double bonds (C=C stretch, $=CH_2$ wag, and $=CH_2$ twist) which are replaced by a peak at 747 cm^{-1} attributed to $-CH_2-$ twist. These changes are consistent with conventional polymerization taking place at the C=C double bond. As noted for XPS, there were no discernible differences in the infrared spectra for silica loadings up to 2.4 wt %. A high level of bulk polymer functional group structural retention is evident from the infrared spectra (which analyses the entire coating thickness) and is consistent with residual plasma-induced modification/damage upon termination of the deposition process being localized to the surface (as seen by XPS, which probes only the outermost 5 nm[40]).

Transmission electron microscopy of the atomized spray plasma deposited 2-hydroxyethyl methacrylate −1 wt % methacryloyl functionalized silica mixture clearly shows clusters of silica nanoparticles (average diameter 15 nm) embedded within the poly(2-hydroxyethyl methacrylate) host matrix, Figure 4.

Deposition rates for the atomized spray plasma deposited poly(2-hydroxyethyl methacrylate)−silica layers were 3.7 ± 0.4 $\mu m\ min^{-1}$ and found to be independent of methacryloyl functionalized silica loading. Precursor mixtures exceeding 2.4 wt % silica content were found to be too viscous to atomize, and therefore unable to be deposited.

Raman spectroscopy showed that the atomized spray plasma deposited poly(2-hydroxyethyl methacrylate)−silica coatings are able to penetrate between two overlapping glass substrates to an inward depth of 743 ± 53 μm, Figure 5. This phenomenon can be attributed to the liquid precursor droplets hitting the surface and wetting into the joint. Given that initiation of polymerization is triggered during the flight of the droplets through the plasma via electrical discharge excitation, then conventional polymerization mechanisms will continue to proceed following impingement onto the surface/joint interface. Optical microscopy showed that there was no statistically significant difference in the coating thickness along the depth of penetration into the joint (which is consistent with the Raman intensity).

3.2. Adhesion of Overlapping Joints. The adhesive bond strength of the overlapping glass joints following atomized spray plasma deposition of poly(2-hydroxyethyl methacrylate) in the absence of methacryloyl functionalized silica content was 5.1 MPa, which rose rapidly with increasing silica loading to reach a maximum value of approximately 84 MPa at 0.5 wt % silica concentration at which point the adherent (bulk glass) failed, Figure 6. At lower silica loadings, weaker failure occurs because of cohesive failure (i.e., the coating itself breaking), while at higher silica content, the bond strength drops reaching 9.8 MPa at 2.4 wt % silica content, which is due to adhesive bond failure (i.e., the coating coming away from the glass-coating interface). This trend is consistent with the methacryloyl modified silica particles acting as cross-linkers, which enhance the coating strength (i.e., a move from cohesive fracture of the adhesive to adhesive failure—the coating coming away from the glass). Above 0.5 wt % silica content, the bond strength starts to fall due to it becoming more difficult to form Si−O−C bonds between the hydroxyl groups present on the glass surface and those contained in the poly(2-hydroxyethyl methacrylate) coating via condensation reactions because the larger extent of bulk cross-linking leads to a drop in polymer chain mobility.[42]

Shear moduli values obtained from lap shear tests gave 0.35 GPa for atomized spray plasma deposited poly(2-hydroxyethyl methacrylate) coatings containing no silica, and this value rose linearly with silica content before leveling off at around 6 GPa for silica loading exceeding 1 wt %, Figure 7. This trend is also consistent with the methacryloyl-modified silica particles inducing greater cross-linking within the bulk films and therefore greater stiffness (shear modulus).

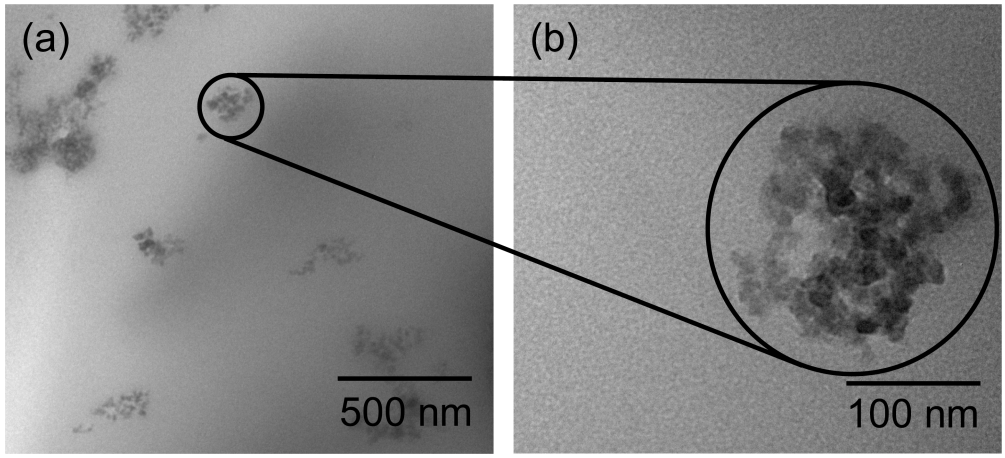

Figure 4. Transmission electron microscopy cross-section images for atomized spray plasma deposited poly(2-hydroxyethyl methacrylate) − 1 wt % methacryloyl functionalized silica at magnification of: (a) ×25 000; and (b) ×130 000.

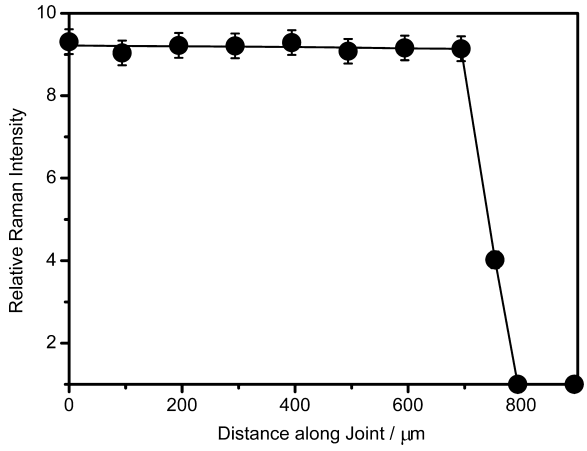

Figure 5. Raman intensity relative to background of the 900−950 cm^{-1} C−C skeletal stretch peaks versus the penetration distance of the atomized spray plasma deposited poly(2-hydroxyethyl methacrylate)−1 wt % methacryloyl functionalized coating for overlapping glass substrates.

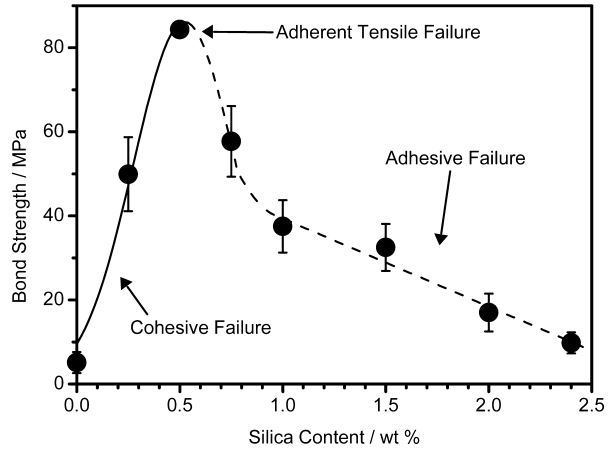

Figure 6. Lap shear bond strengths of atomized spray plasma deposited poly(2-hydroxyethyl methacrylate) bonded glass−glass overlap joints as a function of methacryloyl functionalized silica nanoparticle loading. Solid line denotes cohesive failure and dashed line denotes adhesive failure.

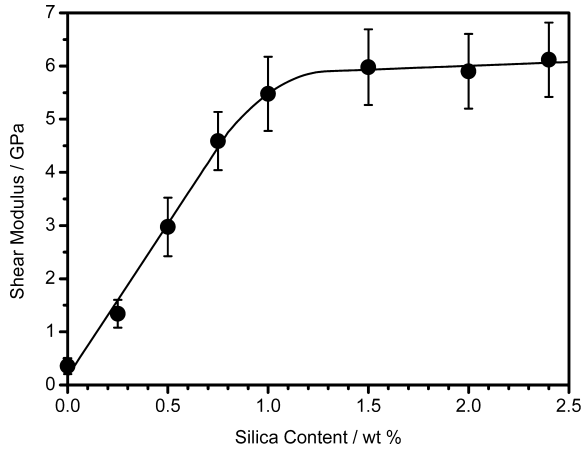

Figure 7. Lap shear moduli of atomized spray plasma deposited poly(2-hydroxyethyl methacrylate) onto glass−glass overlap joints as a function of methacryloyl functionalized silica nanoparticle loading.

4. DISCUSSION

Previous approaches for preparing inorganic-polymer nanocomposites have entailed wet chemical syntheses, which involve multiple steps,[2] high temperatures,[20] and normally require solvent extraction as well as a separate casting step.[26] In contrast, atomized spray plasma deposition (ASPD) utilizes a precursor−nanoparticle slurry mixture for a single-step direct application. An additional advantage of the atomized spray plasma is that deposition rates are vastly enhanced compared to conventional vapor-phase plasma polymerization (by a factor exceeding 250),[43] which is due to the high throughput of precursor delivery into the plasma excitation zone. The depositions rates measured in the present study exceed other dry deposition processes, such as initiated chemical vapor deposition (110 nm min^{-1} for the same monomer[44]).

2-hydroxyethyl methacrylate monomer contains polar bonds (e.g., the hydroxyl group) which are capable of interacting favorably with silica surfaces (Si−OH groups), and therefore plasma-activated precursor mixture droplets during atomized spray plasma deposition are able to wick into the small gap between two overlapping substrates. The lap shear bond strength (84 MPa) of the optimum poly(2-hydroxyethyl methacrylate)−silica nanocomposite prepared in the present

dx.doi.org/10.1021/am402731x | ACS Appl. Mater. Interfaces 2013, 5, 9678−9683

study significantly exceeds those of conventional poly(2-hydroxyethyl methacrylate) based adhesives (10−45 MPa).[45−51] These much higher bond strengths can be attributed to the poly(2-hydroxyethyl methacrylate) hydroxyl groups undergoing condensation reactions with glass surface hydroxyl groups to create Si−O−C bonds at the glass-coating interface.[42] In addition, the methacryloyl groups present on the silica particles help to enhance the adhesive bond strength by acting as cross-linkers within the bulk poly(2-hydroxyethyl methacrylate) thus raising its stiffness (in combination with the mechanical robustness of the incorporated silica nanoparticles), which is illustrated by the rise in shear modulus of the coatings from 0.35 to 6 GPa, Figure 7. An increase in shear modulus with cross-link density has previously been shown to be linear in relationship.[52]These stiffness values are comparable to those reported previously for conventional poly(2-hydroxyethyl methacrylate)−silica nanocomposites.[53] Finally, the outlined atomized spray plasma deposition approach is capable of performing in situ bonding at room temperature via penetration between overlapping glass or silicon substrates. This approach is far more simplistic and straightforward compared to existing methods for bonding glass or silicon (such as anodic bonding[54] requiring high substrate temperatures,[55] or the incorporation of metallic interlayers[56]).

5. CONCLUSIONS

Poly(2-hydroxyethyl methacrylate)−silica nanocomposite layers have been synthesized by a single-step, solventless atomized spray plasma deposition process using a precursor mixture of 2-hydroxyethyl methacrylate and methacryloyl functionalized 15 nm silica nanoparticles. Excellent adhesion and mechanical strength is measured following in situ application to overlapping joints.

AUTHOR INFORMATION

Corresponding Author

*E-mail: j.p.badyal@durham.ac.uk.

Notes

The authors declare no competing financial interest.

ACKNOWLEDGMENTS

The authors thank Evonik Industries AG for the supply of R711 methacryloyl functionalized silica nanoparticles and Tracey Davey at Newcastle University Electron Microscopy Services for assistance with TEM imaging. T.J.W. thanks Surface Innovations Ltd. for financial support.

REFERENCES

(1) Denizli, A.; Say, R.; Patır, S.; Arıca, M. Y. *React. Funct. Polym.* **2000**, *43*, 17−24.
(2) Hung, C.-H.; Whang, W.-T. *J. Mater. Chem.* **2005**, *15*, 267−274.
(3) Yu, Z.; Chen, L.; Chen, S. *J. Mater. Chem.* **2010**, *20*, 6182−6188.
(4) Stupp, S. I.; Braun, P. V. *Science* **1997**, *277*, 1242−1248.
(5) Song, J.; Saiz, E.; Bertozzi, C. R. *J. Am. Chem. Soc.* **2003**, *125*, 1236−1243.
(6) Song, J.; Malathong, V.; Bertozzi, C. R. *J. Am. Chem. Soc.* **2005**, *127*, 3366−3372.
(7) von Werne, T. A.; Germack, D. S.; Hagberg, E. C.; Sheares, V. V.; Hawker, C. J.; Carter, K. R. *J. Am. Chem. Soc.* **2003**, *125*, 3831−3838.
(8) Moran, I. W.; Briseno, A. L.; Loser, S.; Carter, K. R. *Chem. Mater.* **2008**, *20*, 4595−4601.
(9) Bin Hasan Susan, Md. A.; Kanaeko, T.; Noda, A.; Watanabe, M. *J. Am. Chem. Soc.* **2005**, *127*, 4976−4983.
(10) Heredia, K. L.; Bontempo, D.; Ly, T.; Byers, J. T.; Halstenberg, S.; Maynard, H. D. *J. Am. Chem. Soc.* **2005**, *127*, 16955−16960.
(11) Folkman, J.; Moscona, A. *Nature* **1978**, *273*, 345−349.
(12) Schafer, Z. T.; Grassian, A. R.; Song, L.; Jiang, Z.; Gerhart-Hines, Z.; Irie, H. Y.; Gao, S.; Puigserver, P.; Brugge, J. S. *Nature* **2009**, *461*, 109−113.
(13) Villa-Diaz, L. G.; Nandivada, H.; Ding, J.; Nogueira-de-Souza, N. C.; Krebsbach, P. H.; O'Shea, K. S.; Lahann, J.; Smith, G. D. *Nat. Biotechnol.* **2010**, *28*, 581−583.
(14) Chung, M.-H.; Chen, C.-M.; Hsieh, T.-E.; Tang, R.-M.; Tsai, Y. S.; Chu, W.-P.; Liu, M. O.; Juang, F.-S. *Jpn. J. Appl. Phys.* **2009**, *48*, 04C177.
(15) Smetana, K.; Sulc, J.; Krcova, Z.; Pitrova, S. *J. Biomed. Mater. Res.* **1987**, *21*, 1247−1253.
(16) Di Renzo, M.; Ellis, T. H.; Domingue, A.; Bertrand, L.; Sacher, E.; Stangel, I. *J. Adhes.* **1994**, *47*, 115−121.
(17) Young, A. M.; Ho, S. M.; Abou Neel, E. A.; Ahmed, I.; Barralet, J. E.; Knowles, J. C.; Nazhat, S. N. *Acta Biomater.* **2009**, *5*, 2072−2083.
(18) Guvendiren, M.; Heiney, P. A.; Yang, S. *Macromolecules* **2009**, *42*, 6606−6613.
(19) Ji, X. L.; Jiang, X. P.; Diu, X. P.; Dong, D. W.; Yu, D. H.; Jiang, B. Z. *J. Appl. Polym. Sci.* **2003**, *88*, 3168−3175.
(20) Li, S.; Shah, A.; Hsieh, A. J.; Haghighat, R.; Praveen, S. S.; Mukherjee, I.; Wei, E.; Zhang, Z.; Wei, Y. *Polymer* **2007**, *48*, 3982−3989.
(21) Costantini, A.; Luciani, G.; Silvestri, B.; Tescione, F.; Branda, F. *J. Biomed. Mater. Res., Part B* **2008**, *86B*, 98−104.
(22) Xiang, Y.; Peng, Z.; Chen, D. *Eur. Polym. J.* **2006**, *42*, 2125−2132.
(23) Bosch, P.; Del Monte, F.; Mateo, J. L.; Levy, D. *J. Polym. Sci., Part A: Polym. Chem.* **1996**, *34*, 3289−3296.
(24) Liu, Y.-Y.; Liu, D.-M.; Chen, S.-Y.; Tung, T.-H.; Liu, T.-Y. *Acta Biomater.* **2008**, *4*, 2052−2058.
(25) Du, Y.-Z.; Tomohiro, T.; Kodaka, M. *Macromolecules* **2004**, *37*, 803−812.
(26) Cao, Z.; Walter, C.; Landfester, K.; Wu, Z.; Ziener, U. *Langmuir* **2011**, *27*, 9849−9859.
(27) Sun, L.; Dai, J.; Baker, G. L.; Bruening, M. L. *Chem. Mater.* **2006**, *18*, 4033−4039.
(28) Oral, A.; Shahwan, T.; Güler, C. *J. Mater. Res.* **2008**, *23*, 3316−3322.
(29) Gröhn, F.; Kim, G.; Bauer, B. J.; Amis, E. J. *Macromolecules* **2001**, *34*, 2179−2185.
(30) Xiang, Y.; Chen, D. *Eur. Polym. J.* **2007**, *43*, 4178−4187.
(31) Benlikaya, R.; Alkan, M.; Kaya, I. *Polym. Compos.* **2009**, *30*, 1585−1594.
(32) Yasuda, H. In *Plasma Polymerization*; Academic Press: New York, 1985; p 4.
(33) Ryan, M. E.; Hynes, A. M.; Badyal, J. P. S. *Chem. Mater.* **1996**, *8*, 37−42.
(34) Friedrich, J. *Plasma Processes Polym.* **2011**, *8*, 783−802.
(35) Ward, L. J.; Schofield, W. C. E.; Badyal, J. P. S.; Goodwin, A. J.; Merlin, P. J. *Langmuir* **2003**, *19*, 2110−2114.
(36) Ward, L. J.; Schofield, W. C. E.; Badyal, J. P. S.; Goodwin, A. J.; Merlin, P. J. *Chem. Mater.* **2003**, *15*, 1466−1469.
(37) Friedman, R. M.; Hudis, J.; Perlman, M. L. *Phys. Rev. Lett.* **1972**, *29*, 692−695.
(38) Evans, J. F.; Gibson, J. H.; Moulder, J. F.; Hammond, J. S.; Goretzki, H. *Fresenius J. Anal. Chem.* **1984**, *319*, 841−844.
(39) Lin-Vien, D.; Colthup, N. B.; Fateley, W. G.; Grasselli, J. G. In *The Handbook of Infrared and Raman Characteristic Frequencies of Organic Molecules*; Academic Press: London, 1991; p 11.
(40) Klasson, M.; Hedman, J.; Berndtsson, A.; Nilsson, R.; Nordling, C.; Melnik, P. *Phys. Scr.* **1972**, *5*, 93−95.
(41) Lin-Vien, D.; Colthup, N. B.; Fateley, W. G.; Grasselli, J. G. In *The Handbook of Infrared and Raman Characteristic Frequencies of Organic Molecules*; Academic Press: London, 1991; p 137.
(42) Xu, P.; Wang, H.; Tong, R.; Iv, R.; Shen, Y.; Du, Q.; Zhong, W. *Polym. Degrad. Stab.* **2006**, *91*, 1522−1529.

(43) Tarducci, C.; Schofield, W. C. E.; Brewer, S. A.; Willis, C.; Badyal, J. P. S. *Chem. Mater.* **2002**, *14*, 2541−2545.
(44) Chan, K.; Gleason, K. K. *Langmuir* **2005**, *21*, 8930−8939.
(45) Stackhouse, J. A., Jr.; Kristol, D. S.; Von Hagen, S.; Rao, G. *J. Biomed. Mater. Res.* **1989**, *23*, 81−90.
(46) Chigira, H.; Koike, T.; Hasegawa, T.; Itoh, K.; Wakumoto, S.; Hayakawa, T. *Dent. Mater. J.* **1989**, *8*, 86−92.
(47) Causton, B.; Sefton, J. *Br. Dent. J.* **1989**, *167*, 308−311.
(48) Perdigão, J.; Swift, E. J., Jr.; Heymann, H. O.; Malek, M. A. *Am. J. Dent.* **1998**, *11*, 207−213.
(49) Chappelow, C. C.; Power, M. D.; Bowles, C. Q.; Miller, R. G.; Pinzino, C. S.; Eick, J. D. *Dent. Mater.* **2000**, *16*, 396−405.
(50) Hussain, L. A.; Dickens, S. H.; Bowen, R. L. *Biomaterials* **2005**, *26*, 3973−3979.
(51) Walter, R.; Swift, E. J., Jr.; Ritter, A. V.; Bartholomew, W. W.; Gibson, C. G. *Am. J. Dent.* **2009**, *22*, 215−218.
(52) Head, D. A.; Levine, A. J.; MacKintosh, F. C. *Phys. Rev. Lett.* **2003**, *91*, 108102.
(53) Kaddami, H.; Gerard, J. F.; Hajji, P.; Pascault, J. P. *J. Appl. Polym. Sci.* **1999**, *73*, 2701−2713.
(54) Pomerantz, D. I. *Anodic Bonding*. U.S. Patent 3 397 278, 1968.
(55) Anthony, T. R. *J. Appl. Phys.* **1985**, *58*, 1240−1247.
(56) Lang, G. F., Jr. *Bonding of Semiconductor Devices to Substrates*. U.S. Patent 3 316 628, 1967.